Available online at www.sciencedirect.com
ScienceDirect
Mendeleev Commun., 2010, **20**, 340–342
Mendeleev Communications

Potential energy surface and rate constant of the inversion substitution reactions $CH_3X + O_2 \rightarrow CH_3O_2^{\bullet} + X^{\bullet}$ (X = SH, NO_2)

Anton S. Nizovtsev[a] and Alexey V. Baklanov*[a,b]

[a] *Institute of Chemical Kinetics and Combustion, Siberian Branch of the Russian Academy of Sciences, 630090 Novosibirsk, Russian Federation. Fax: +7 383 330 7350; e-mail: baklanov@kinetics.nsc.ru*
[b] *Department of Physics, Novosibirsk State University, 630090 Novosibirsk, Russian Federation*

DOI: 10.1016/j.mencom.2010.11.013

The temperature dependence of the rate constant of the inversion substitution reactions $CH_3X + O_2 \rightarrow CH_3O_2^{\bullet} + X^{\bullet}$ (X = SH, NO_2) can be expressed as $k = 6.8\times10^{-12}(T/1000)^{1.49}\exp(-62816 \text{ cal mol}^{-1}/RT) \text{ cm}^3 \text{ s}^{-1}$ (X = SH) and $k = 6.8\times10^{-12}(T/1000)^{1.26}\times\exp(-61319 \text{ cal mol}^{-1}/RT) \text{ cm}^3 \text{ s}^{-1}$ (X = NO_2), as found with the use of high-level quantum chemical methods and the transition state theory.

The new mechanism of the homolytic inversion substitution by oxygen $RX + O_2 \rightarrow RO_2^{\bullet} + X^{\bullet}$ with the substrates RX = CH_4, SiH_4, CH_3Br, CF_3Br, CH_3I and SiH_3I has been studied recently within the approach combining the methods of quantum chemistry and the transition state theory.[1] For several substrates, it has been shown that the bimolecular substitution reaction competes with traditional bimolecular mechanism[2] of hydrogen abstraction by molecular oxygen $R'H + O_2 \rightarrow R'^{\bullet} + HO_2^{\bullet}$ and so provides the new initiation mechanism for the chain oxidation process. An activation barrier for the inversion substitution correlates with the value of reaction endothermicity.[1(c)] Therefore, this mechanism is competitive in the case of relatively weakly bound leaving X group.

In the cited studies, the reactions with an atom (X = H, Br and I) as a leaving group were considered. It is of great interest to estimate the contribution of the inversion substitution reactions $RX + O_2 \rightarrow RO_2^{\bullet} + X^{\bullet}$, where the molecular fragment is a leaving group since the reactions of this type can be widely spread in the environment due to high oxygen concentration.

Here, we investigated substitution reactions with thiol (SH) and nitro (NO_2) groups as the leaving ones by quantum chemical and transition state theory calculations:

$$CH_3SH + O_2 \rightarrow CH_3O_2^{\bullet} + SH^{\bullet} \quad (1)$$

$$CH_3NO_2 + O_2 \rightarrow CH_3O_2^{\bullet} + NO_2^{\bullet} \quad (2)$$

The dissociation energies of 74.7±1.0 and 62.3±0.5 kcal mol^{-1} for the bonds C–S (CH_3SH) and C–N (CH_3NO_2), respectively,[3] are essentially lower than the C–H (CH_4) bond energy (105.0±0.1 kcal mol^{-1}).[3] This fact allowed us to expect the substitution reactions to be competitive with bimolecular hydrogen abstraction reactions. The choice of reaction (1) for the study is due to the presence of SH-containing compounds in the living organisms, where the thiol group is a part of cysteine amino acid in the proteins. We consider reaction (1) as a model for the substitution reactions of oxygen with SH-containing substrates in biosystems. Nitromethane (CH_3NO_2) is the simplest member of the series of nitro compounds being high-energy substances. Nitromethane reactions with oxygen are important for estimating their stability in the molecular oxygen environment.

The present work is aimed at the study of the energy profiles of reactions (1) and (2) with the use of high-level quantum chemical methods to calculate rate constant temperature dependences for both substitution reactions (1) and (2) and the reverse ones within the transition state theory.

In order to illustrate the accuracy of the proposed theoretical approach,[†] we calculated bond dissociation energies (BDEs) for bonds formed or broken during the reactions (Table 1). The BDEs calculated are in excellent agreement with the experimental values also presented in Table 1. This allows us to expect similar accuracy at a level of 1 kcal mol^{-1} in the calculations of energy barriers.

The transition states (TSs) found for substitution reactions (Figure 1) have single imaginary frequency and connect the products and reagents of corresponding reactions as intrinsic reaction coordinate (IRC) analysis shows. The other stationary points on a potential energy surface (PES) possess real vibrational frequencies only. The calculated vibrational wavenumbers and rotational constants of compounds involved in substitution reactions are presented in Table 2. The calculated vibrational wavenumbers are in a good agreement with the experimental data.

In the transition states, the distances between the central atom C and the nearest atom of the arriving (O_2) and leaving

[†] Geometric parameters of reagents, products and transition states were fully optimized by the MP2(fc) method[4] with Dunning's correlation-consistent basis set of triple-zeta quality with additional *d*-functions, cc-pV(T+*d*)Z, on sulfur and cc-pVTZ basis sets[5] on the all remaining elements (next the combination of these basis sets is abbreviated as VTZ). All the following single-point calculations were carried out with MP2/VTZ geometries.

In order to calculate correlation of valence electrons, the coupled-cluster method [CCSD(T)][6] was applied within frozen core approximation. Energetic properties of the processes being considered were calculated with the use of complete basis set (CBS) extrapolation technique by two-parameter extrapolation formula:[7] $E(n) = E_{CCSD(T)/CBS} + B/n^3$. Energy values calculated with VTZ and VQZ basis sets (n = 3, 4) were used for this extrapolation.

The correlation of the core electrons (E_{core}) was calculated at the MP2/cc-pwCVTZ level.[8] These effects were determined as the difference between the energy values obtained without (all-electron correlation) and with frozen core approximation. Scalar relativistic corrections (E_{SR}) were computed as the difference between MP2(DKH)/cc-pVTZ-DK and MP2/cc-pVTZ energies.[9] The spin-orbit correction (E_{SO}) for $^2\Pi_{3/2}$ state of SH radical (–0.48 kcal mol^{-1}) was taken from ref. 10. Zero-point vibrational energies (E_{ZPE}) were calculated from the MP2/VTZ harmonic vibrational frequencies without scaling factors. The thermal correction to the enthalpy (E_{TC}) was calculated within rigid-rotor-harmonic-oscillator approximation and used for obtaining reaction enthalpies at 298 K. Only for the highest vibrational wavenumber of NO_2, the experimental value instead of the calculated one was used in all corresponding energy and kinetic calculations because of the poor MP2/VTZ result.

For all open-shell species the calculations were spin-unrestricted.

The calculations were performed with the use of Gaussian 03 program package.[11] Some basis sets were taken from the EMSL database.[12]

Table 1 Comparison of experimental and calculated BDEs (kcal mol^{-1}).

Bond	$\Delta E_{CCSD(T)/CBS}$	ΔE_{ZPE}	ΔE_{TC}	ΔE_{core}	ΔE_{SR}	ΔE_{SO}	$D(0\ K)_{calc}$	$D(298\ K)_{calc}$	$D(298\ K)_{exp}$
$HO_2^{\bullet} \rightarrow H^{\bullet} + O_2$	55.25	–7.05	–5.88	0.20	–0.13	0.00	48.3	49.4	49.16±0.06[a]
$CH_3SH \rightarrow {}^{\bullet}CH_3 + SH^{\bullet}$	79.73	–6.38	–4.62	0.47	–0.23	–0.48	73.1	74.9	74.7±1.0[a]
$CH_3O_2^{\bullet} \rightarrow {}^{\bullet}CH_3 + O_2$	36.59	–6.46	–4.86	0.22	–0.13	0.00	30.2	31.8	32.7±0.9[a]
$CH_3NO_2 \rightarrow {}^{\bullet}CH_3 + NO_2^{\bullet}$	67.04	–7.40	–5.76	0.29	–0.13	0.00	59.8	61.5	62.3±0.5[a]

[a]Recommended values from ref. 3.

Table 2 Rotational constants and vibrational wavenumbers for species from the substitution reactions calculated at the MP2/VTZ level (experimental values are given in parentheses).

Species	Rotational constants/cm^{-1}	Vibrational wavenumbers[a]/cm^{-1}
O_2	1.406	1454 (1580)[b]
CH_3SH	3.471, 0.434, 0.416	245, 739 (710),[c] 812 (802),[c] 986 (956),[c] 1106 (1072),[c] 1367 (1332),[c] 1493 (1444),[c] 1507 (1453),[c] 2777 (2605),[c] 3097 (2948),[c] 3198 (3012),[c] 3200 (3015)[c]
$SH^{\bullet}$	9.666	2768 (2712)[b]
$CH_3O_2^{\bullet}$	1.764, 0.387, 0.338	130 (170±8),[d] 505 (482±9),[e] 963 (902),[f] 1153 (1117±2),[d] 1206 (1183),[d] 1283, 1466 (1408),[d] 1499 (1441),[d] 1512 (1453±2),[d] 3105 (2954),[d] 3219 (3020±2),[d] 3226 (3033)[d]
TS1	1.074, 0.054, 0.052	1934i, 83, 132, 146, 206, 255, 475, 577, 1081, 1102, 1150, 1424, 1428, 1456, 2762, 3167, 3359, 3370
CH_3NO_2	0.407, 0.355, 0.197	32, 482 (475),[g] 610 (603),[g] 678 (657),[g] 947 (918),[g] 1124 (1096),[g] 1148 (1131),[g] 1417 (1380),[g] 1426 (1397),[g] 1489 (1410),[g] 1499 (1434),[g] 1774 (1583),[g] 3122 (2974),[g] 3229 (3045),[g] 3256 (3080)[g]
$NO_2^{\bullet}$	7.907, 0.431, 0.408	771 (750),[h] 1372 (1318),[h] 4192 (1618)[h]
TS2	0.329, 0.043, 0.040	2899i, 20, 81, 147, 159, 216, 379, 411, 542, 742, 1080, 1170, 1203, 1346, 1423, 1424, 1606, 1826, 3171, 3367, 3384

[a]Calculated values are the harmonic vibrational wavenumbers. [b]Gas.[13] [c]Gas.[14] [d]Gas.[15] [e]Gas.[16] [f]Ar matrix.[17] [g]Gas.[18] [h]Gas.[19]

(SH or NO_2) groups are stretched, as compared with the corresponding bonds in the reagents and products. Thus, the C–O bond distance is 1.753 Å in TS1 or 1.767 Å in TS2, which are longer by about 0.3 Å than that in the product $CH_3O_2^{\bullet}$ (1.443 Å). The C–S bond in TS1 (2.335 Å) and the C–N bond in TS2 (2.039 Å) are longer than those in the reagents CH_3SH (1.811 Å) and CH_3NO_2 (1.484 Å).

The calculated activation barriers for inversion substitution reactions (1) and (2) and the reverse ones are given in Table 3. It is worth comparing the obtained activation barrier heights with the values expected on the basis of correlation between E_0 and reaction enthalpy ΔH_0^O derived previously for the substitution reactions $RX + O_2 \rightarrow RO_2^{\bullet} + X^{\bullet}$ with an atom as a leaving group X: $E_0 = \gamma + \delta\Delta H_0^O$ with parameters $\gamma = 8.9$ kcal mol^{-1} and $\delta = 1.11$.[1(c)]

On the basis of this correlation and reaction enthalpies ΔH_0^O given in Table 3, one should expect barrier height values to be 56.5 and 41.8 kcal mol^{-1} for reactions (1) and (2), respectively. However, barrier values (62.8 and 61.3 kcal mol^{-1}) calculated and presented in Table 3 are essentially higher [especially for reaction (2)] than those deduced from a correlation for reactions with an atom as a leaving group.

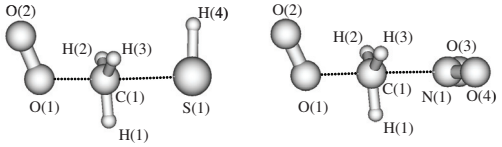

TS1, C_S TS2, C_S

Figure 1 Structures of the transition states for the inversion substitution $CH_3X + O_2 \rightarrow CH_3O_2^{\bullet} + X^{\bullet}$ (X = SH, NO_2) reactions. Selected bond lengths (Å) and angles (°): in TS1: C(1)–O(1) 1.753, C(1)–S(1) 2.335, C(1)–H(1) 1.076, C(1)–H(2) 1.074, O(1)–O(2) 1.226, S(1)–H(4) 1.336, C(1)–O(1)–O(2) 113.9, C(1)–S(1)–H(4) 93.0, O(1)–C(1)–H(1) 95.3, H(1)–C(1)–S(1) 86.6; in TS2: C(1)–O(1) 1.767, C(1)–N(1) 2.039, C(1)–H(1) 1.076, C(1)–H(2) 1.074, O(1)–O(2) 1.215, N(1)–O(3) 1.214, C(1)–O(1)–O(2) 114.3, C(1)–N(1)–O(3) 115.6, O(1)–C(1)–H(1) 94.0, H(1)–C(1)–N(1) 85.4, H(1)–C(1)–N(1)–O(3) 89.5.

We explain this fact by an additional repulsion in transition states between hydrogen atoms of the CH_3 group to be inverted and H and O atoms of SH and NO_2 groups, respectively, which seems to provide an additional raise in the activation barrier height, as compared with the case of an atomic leaving group (see Figure 1). In favour of this hypothesis we should point out that the relative torsional orientation of CH_3 and leaving SH and NO_2 groups in transition states (see Figure 1) just corresponds to the minimum of this repulsion.

This activation energy raise makes substitution reactions noncompetitive, as compared with the hydrogen abstraction reactions

$$CH_3SH + O_2 \rightarrow CH_2SH^{\bullet} + HO_2^{\bullet}\ (\Delta H_{298}^O = 44.74\pm2.06\ \text{kcal mol}^{-1}),^3$$

$$CH_3SH + O_2 \rightarrow CH_3S^{\bullet} + HO_2^{\bullet}\ (\Delta H_{298}^O = 38.24\pm0.56\ \text{kcal mol}^{-1}),^3$$

$$CH_3NO_2 + O_2 \rightarrow CH_2NO_2^{\bullet} + HO_2^{\bullet}\ (\Delta H_{298}^O = 50.14\pm0.06\ \text{kcal mol}^{-1}).^3$$

The previous results of quantum chemical calculations for similar abstraction reaction show that its activation barrier is close to its endothermicity.[20] The above enthalpy values ΔH_{298}^O for these reactions are distinctly smaller than the activation barriers for substitution reactions, which are 62.8 and 61.3 kcal mol^{-1}, respectively (Table 3).

The rate constants for both reactions (1) and (2) and the reverse ones have been calculated within transition state theory formalism for the temperature range of 273–2000 K with a 100 K step in the rigid-rotor-harmonic-oscillator approximation.[21]

A correction for the contribution of tunneling through the potential barrier was estimated with the use of the Wigner equation:[22]

$$F_{tunnel}(T) = 1 + \frac{1}{24}\left(\frac{ih\nu^{\neq}}{k_B T}\right)^2,$$

where $\nu^{\neq}$ is the imaginary vibrational frequency of TS.

Table 3 Calculated reaction barrier E_0, enthalpy ΔH_0^O at 0 K, enthalpy ΔH_{298}^O at 298 K and the temperature dependences of rate constants $k(T)$ (experimental values are given in parentheses).

Reaction	E_0/kcal mol^{-1}	ΔH_0^O/kcal mol^{-1}	ΔH_{298}^O/kcal mol^{-1}	$k(T)$/cm^3 s^{-1}
$CH_3SH + O_2 \rightarrow CH_3O_2^{\bullet} + SH^{\bullet}$	62.8	42.9	43.0 (42.0±1.9)[a]	$k = 6.8\times10^{-12}(T/1000)^{1.49}\exp(-62816\ \text{cal mol}^{-1}/RT)$
$CH_3NO_2 + O_2 \rightarrow CH_3O_2^{\bullet} + NO_2^{\bullet}$	61.3	29.6	29.6 (29.6±1.4)[a]	$k = 6.8\times10^{-12}(T/1000)^{1.26}\exp(-61319\ \text{cal mol}^{-1}/RT)$
$CH_3O_2^{\bullet} + SH^{\bullet} \rightarrow CH_3SH + O_2$	19.9	–42.9	–43.0 (–42.0±1.9)[a]	$k = 2.9\times10^{-12}(T/1000)^{1.39}\exp(-19938\ \text{cal mol}^{-1}/RT)$
$CH_3O_2^{\bullet} + NO_2^{\bullet} \rightarrow CH_3NO_2 + O_2$	31.7	–29.6	–29.6 (–29.6±1.4)[a]	$k = 1.6\times10^{-12}(T/1000)^{1.40}\exp(-31735\ \text{cal mol}^{-1}/RT)$

[a]Recommended values from ref. 3.

Table 3 summarizes the calculated rate constants for substitution reactions (1) and (2) and the reverse ones in the form of modified Arrhenius equations.

Thus, in the present work, we carried out the precise electronic structure calculations by *ab initio* quantum chemical methods, which allow us to obtain detailed information on the thermodynamics and activation barriers for $CH_3SH + O_2 \rightarrow CH_3O_2^{\bullet} + SH^{\bullet}$ and $CH_3NO_2 + O_2 \rightarrow CH_3O_2^{\bullet} + NO_2^{\bullet}$ inversion substitution reactions. The temperature dependence of the rate constants was calculated for the forward and reverse substitution reactions within transition state theory formalism. The raise in an activation barrier height for the substitution reactions $RX + O_2 \rightarrow RO_2^{\bullet} + X^{\bullet}$ with a molecular fragment as a leaving group X, as compared with the case of an atomic leaving group with similar endothermicity, was established. We suppose that the reason for the increase is the rise of CH_3 group inversion barrier owing to repulsion between its hydrogen atoms and leaving group atoms in the transition state.

On the basis of the results and previously published data,[1] we can conclude that the inversion substitution reactions with molecular oxygen $ZH_3Y + O_2 \rightarrow ZH_3O_2^{\bullet} + Y^{\bullet}$ are competitive with a bimolecular abstraction reaction for the substrates ZH_3Y with carbon as a central atom (Z = C), when the leaving group Y is a rather weakly bound atom (Y = Br, I). The replacement of hydrogen atoms in the ZH_3 group by bulkier atoms or groups leads to an essential activation barrier rise and thus makes the contribution of substitution reaction negligible. The same result takes place when the leaving group is a molecular fragment.

This work was supported by the Russian Foundation for Basic Research (grant no. 09-03-00310-a) and the programme of the Russian Government 'Research and educational personnel of innovative Russia' (contract no. 14.740.11.0722). The computing time on an NKS-160 cluster has been provided by the Siberian Supercomputer Center.

References

1 (*a*) G. A. Bogdanchikov, A. V. Baklanov and D. H. Parker, *Chem. Phys. Lett.*, 2004, **385**, 486; (*b*) G. A. Bogdanchikov, A. V. Baklanov and D. H. Parker, *Izv. Akad. Nauk, Ser. Khim.*, 2008, 1803 (*Russ. Chem. Bull., Int. Ed*., 2008, **57**, 1837); (*c*) A. S. Nizovtsev, G. A. Bogdanchikov and A. V. Baklanov, *Combust. Flame*, 2010, **157**, 1382.

2 (*a*) J. Warnatz, in *Combustion Chemistry*, ed. W. C. Gardiner, Springer-Verlag, New York, 1984, p. 197; (*b*) E. T. Denisov and T. G. Denisova, *Usp. Khim*., 2002, **71**, 477 (*Russ. Chem. Rev.*, 2002, **71**, 417).

3 Y.-R. Luo, *Comprehensive Handbook of Chemical Bond Energies*, CRC Press, Taylor and Francis Group, Boca Raton, FL, 2007.

4 C. Møller and M. S. Plesset, *Phys. Rev.*, 1934, **46**, 618.

5 (*a*) T. H. Dunning, Jr., *J. Chem. Phys.*, 1989, **90**, 1007; (*b*) T. H. Dunning, Jr., K. A. Peterson and A. K. Wilson, *J. Chem. Phys.*, 2001, **114**, 9244.

6 (*a*) G. D. Purvis III and R. J. Bartlett, *J. Chem. Phys.*, 1982, **76**, 1910; (*b*) K. Raghavachari, G. W. Trucks, J. A. Pople and M. Head-Gordon, *Chem. Phys. Lett.*, 1989, **157**, 479.

7 T. Helgaker, W. Klopper, H. Koch and J. Noga, *J. Chem. Phys.*, 1997, **106**, 9639.

8 K. A. Peterson and T. H. Dunning, Jr., *J. Chem. Phys.*, 2002, **117**, 10548.

9 (*a*) M. Douglas and N. M. Kroll, *Ann. Phys. (NY)*, 1974, **82**, 89; (*b*) B. A. Hess, *Phys. Rev. A*, 1985, **32**, 756; (*c*) B. A. Hess, *Phys. Rev. A*, 1986, **33**, 3742; (*d*) W. A. de Jong, R. J. Harrison and D. A. Dixon, *J. Chem. Phys.*, 2001, **114**, 48.

10 Q. K. Timerghazin, G. H. Peslherbe and A. M. English, *Phys. Chem. Chem. Phys*., 2008, **10**, 1532.

11 M. J. Frisch, G. W. Trucks, H. B. Schlegel, G. E. Scuseria, M. A. Robb, J. R. Cheeseman, J. A. Montgomery, Jr., T. Vreven, K. N. Kudin, J. C. Burant, J. M. Millam, S. S. Iyengar, J. Tomasi, V. Barone, B. Mennucci, M. Cossi, G. Scalmani, N. Rega, G. A. Petersson, H. Nakatsuji, M. Hada, M. Ehara, K. Toyota, R. Fukuda, J. Hasegawa, M. Ishida, T. Nakajima, Y. Honda, O. Kitao, H. Nakai, M. Klene, X. Li, J. E. Knox, H. P. Hratchian, J. B. Cross, V. Bakken, C. Adamo, J. Jaramillo, R. Gomperts, R. E. Stratmann, O. Yazyev, A. J. Austin, R. Cammi, C. Pomelli, J. W. Ochterski, P. Y. Ayala, K. Morokuma, G. A. Voth, P. Salvador, J. J. Dannenberg, V. G. Zakrzewski, S. Dapprich, A. D. Daniels, M. C. Strain, O. Farkas, D. K. Malick, A. D. Rabuck, K. Raghavachari, J. B. Foresman, J. V. Ortiz, Q. Cui, A. G. Baboul, S. Clifford, J. Cioslowski, B. B. Stefanov, G. Liu, A. Liashenko, P. Piskorz, I. Komaromi, R. L. Martin, D. J. Fox, T. Keith, M. A. Al-Laham, C. Y. Peng, A. Nanayakkara, M. Challacombe, P. M. W. Gill, B. Johnson, W. Chen, M. W. Wong, C. Gonzalez and J. A. Pople, *Gaussian 03, Revision E.01*, Gaussian, Inc., Wallingford CT, 2004.

12 EMSL basis set library, http://www.emsl.pnl.gov/forms/basisform.html.

13 K. P. Huber and G. Herzberg, *Molecular Spectra and Molecular Structure, Constants of Diatomic Molecules*, Van Nostrand Reinhold, New York, 1979, vol. 4.

14 H. B. Schlegel, S. Wolfe and F. Bernardi, *J. Chem. Phys*., 1977, **67**, 4181.

15 D.-R. Huang, L.-K. Chu, Y.-P. Lee, H.-Y. Liao, E.N. Sharp, P. Rupper and T. A. Miller, *J. Chem. Phys*., 2007, **127**, 044311.

16 S. J. Blanksby, T. M. Ramond, G. E. Davico, M. R. Nimlos, S. Kato, V. M. Bierbaum, W. C. Lineberger, G. B. Ellison and M. Okumura, *J. Am. Chem. Soc*., 2001, **123**, 9585.

17 S. Nandi, S. J. Blanksby, X. Zhang, M. R. Nimlos, D. C. Dayton and G. B. Ellison, *J. Phys. Chem. A*, 2002, **106**, 7547.

18 D. Gorse, D. Cavagnat, M. Pesquer and C. Lapouge, *J. Phys. Chem. A*, 1993, **97**, 4262.

19 T. Shimanouchi, *J. Phys. Chem. Ref. Data*, 1972, **1**, 189.

20 N. K. Srinivasan, J. V. Michael, L. B. Harding and S. J. Klippenstein, *Combust. Flame*, 2007, **149**, 104.

21 E. E. Nikitin, *Theory of Elementary Atomic and Molecular Processes in Gases*, Clarendon Press, Oxford, 1974.

22 E. P. Wigner, *Z. Phys. Chem*., 1932, **B19**, 203.

Received: 15th April 2010; Com. 10/3506